Temperature Solver for Highly Nonlinear Ferromagnetic Materials for Thin Moving Sheets in Transversal Flux Induction Heating

Christoph Monzel and Gerhard Henneberger, *Member, IEEE*

***Abstract*—In this paper, a successive iteration method has been applied to a highly nonlinear temperature problem. The nonlinearity arises from the specific heat of ferromagnetic materials. These materials are heat treated in transversal flux inductive heating devices (TFIH) as thin strips. The convergence behavior is examined and compared to the classical Newton–Raphson scheme. Additionally, a method will be presented which takes phase change energies of the material into account.**

***Index Terms*—FEM, inductive heating, nonlinear, specific heat, temperature.**

I. Introduction

THE NUMERICAL calculation of a transverse flux inductive heating device (TFIH) for heating thin strips is weakly coupled between the electromagnetic eddy-current and the instationary thermal problem. The nonlinear electromagnetic eddycurrent problem for ferromagnetic strip materials is solved with a Boundary Impedance method [1]. The instationary thermal problem causes serious troubles for this group of materials.

A recent application of a TFIH device in industry is the ultrashort annealing of cold rolled steel strip [2]. The steel strip consists of iron, with less than 2% alloying elements. In this application, a very large temperature range of up to 950 °C is crossed. When the numerical simulation of the TFIH device is performed, problems arise from very high peaks of the specific heat at the Curie temperature $\mathbf{T_c}$ (Fig. 1). Also, the phase changes $\alpha - \gamma$ and $\gamma - \delta$ lead to a saltus in the specific heat [4] caused by changes in the crystal structure. This is caused by the definition of the specific heat $c_p = dQ/d\vartheta$, and the fact that the internal energy Q rises while the temperature ϑ remains constant.

II. Numerical Approach

The well-known time-dependent Fourier temperature equation

$$w = -\mathrm{div}(\lambda \,\mathrm{grad}\,\vartheta) + \rho c_p \frac{d\vartheta}{dt} \tag{1}$$

where w is the heat density, ρ the mass density, and λ the heat conduction coefficient, can be transformed into a stationary equation, since the strip velocity v is constant. The losses which are caused by convection and radiation should be taken into account:

$$w = -\mathrm{div}(\lambda \,\mathrm{grad}\,\vartheta) + \vec{v}\rho c_p \,\mathrm{grad}\,\vartheta + \frac{2\alpha}{d}(\vartheta - \vartheta_a) + \frac{2\epsilon_r B}{d}(\vartheta^4 - \vartheta_a^4) \tag{2}$$

where α is the heat-transfer coefficient for the convectional term, ϵ_r the radiation coefficient, and d the strip thickness. The variable ϑ_a describes the ambient temperature.

In (2), the conduction, transport, and radiation terms are nonlinear. After discretization of the equation system, it can be solved with a BICG solver with an ILU(0) preconditioner and the Newton–Raphson algorithm. The transport term of the equation system is stabilized with an upwinding scheme [3].

The Newton–Raphson algorithm works well as long as the strip temperature is below the Curie temperature, but fails if higher temperatures are reached.

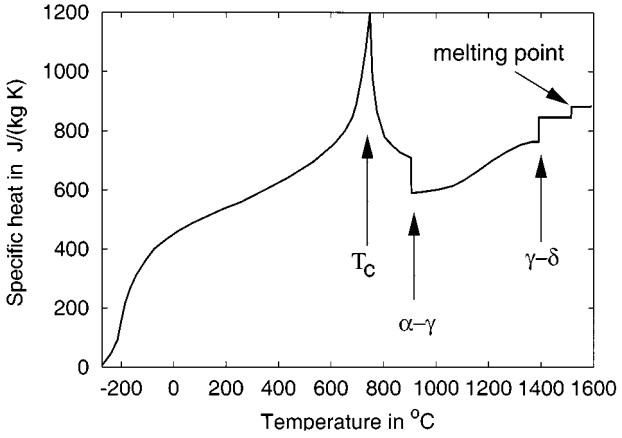

Fig. 1. Specific heat of pure iron.

III. Nonlinear Iterative Methods

The preferred iteration method is the Newton–Raphson scheme because of its quadratic convergence behavior. Several derived methods have been tried without success, such as damping and bounds checking methods. Also, providing a good starting solution for the first iteration step does not help.

Thus, the successive iteration method

$$\mathbf{A}(\mathbf{x}_n) \cdot \mathbf{x}_{n+1} = \mathbf{b} \tag{3}$$

Manuscript received July 5, 2001; revised October 25, 2001.

The authors are with the Department of Electrical Machines, Aachen Institute of Technology (RWTH), Aachen 52056, Germany (e-mail: monzel@iem.rwth-aachen.de; henneberger@rwth-aachen.de).

Publisher Item Identifier S 0018-9464(02)01578-9.

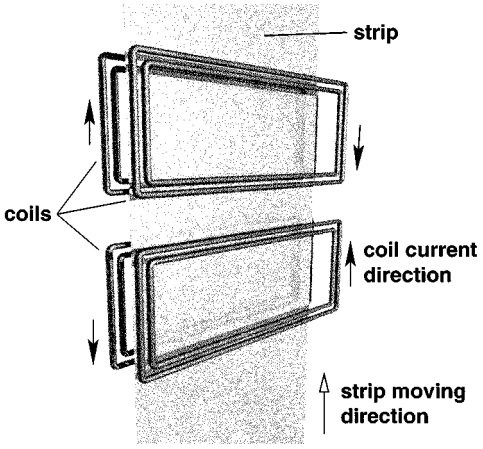

Fig. 2. Example TFIH device.

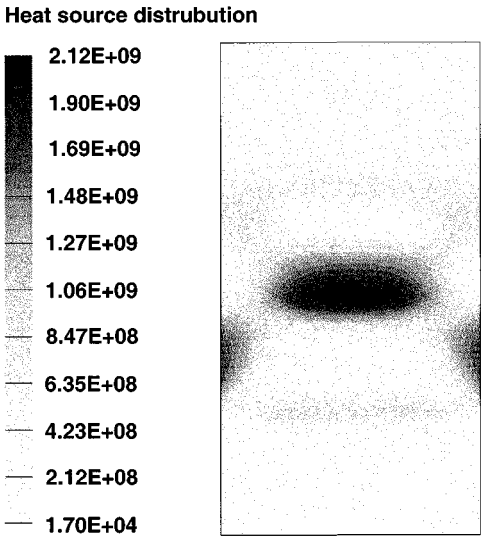

Fig. 3. Heat source distribution in W/m^3.

has been applied, where the system matrix $\mathbf{A}$ is rebuilt with the solution from the previous iteration step.

IV. Example Application

In Fig. 2, an example of a TFIH device with four coils is sketched. One coil consists of two windings. Two coils are located on the front and back side of the strip. The current direction in the front coils matches the one on the back side coils. All currents have the same frequency, value, and phase. For clarity, the yoke is not shown. The strip entries the device with a temperature of 20 °C and is moving upwards.

A typical heat source distribution of this TFIH device is shown in Fig. 3. The strip is moving with a velocity of 4.5 m/min. The induced power into the strip is 136 kW. The strip is 0.5-m wide and 0.8-mm thick. This characteristic heat source distribution has been used in the numerical experiments in the following sections.

Fig. 4 illustrates the resulting temperature distribution. The temperature is in a range of 20 °C to 905 °C. Different temperature ranges can be accessed with one heat source distribution by manipulating the strip velocity.

Fig. 4. Temperature distribution caused by the heat source distribution of Fig. 3 in degrees C.

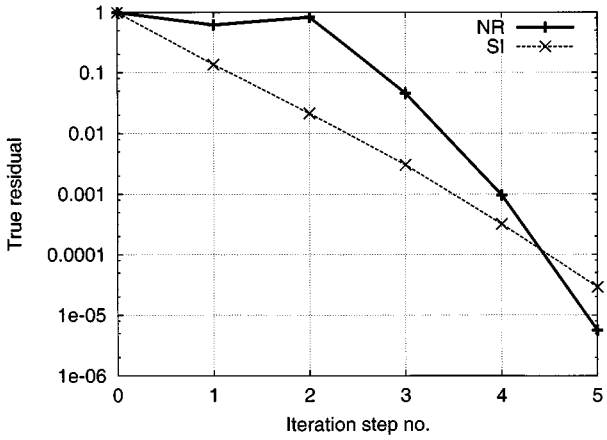

Fig. 5. Convergence behavior of Newton–Raphson (NR) and successive iteration (SI).

V. Convergence Behavior

In Fig. 5, the convergence behavior of the Newton–Raphson (NR) and the successive iteration method are depicted. The strip velocity of the example in Section IV was increased to 7 m/min, while the induced power remains constant. So the temperature of the strip is always below the Curie temperature. As expected, the successive iteration is linear convergent in contrast to the NR method, which is quadratically convergent. The true residual $r_{n_{\mathrm{true}}} = |\mathbf{b_0} - \mathbf{A}(\mathbf{x_n}) \cdot \mathbf{x_n}|/|\mathbf{b_0}|$ of the NR method overshoots in step one, so both methods reach an acceptable tolerance of 10^{-4} in the same iteration step. Thus, the drawback of the linear behavior of the successive iteration is not as great as might be expected.

A. Convergence Criteria

In general, either the true or relative residual is chosen as convergence criteria for the nonlinear iteration loop. For performance reasons, the relative residual $r_{n_{\mathrm{rel}}} = |\mathbf{x_{n-1}} - \mathbf{x_n}|/|\mathbf{x_n}|$ should be used, since this criteria does not require a complete

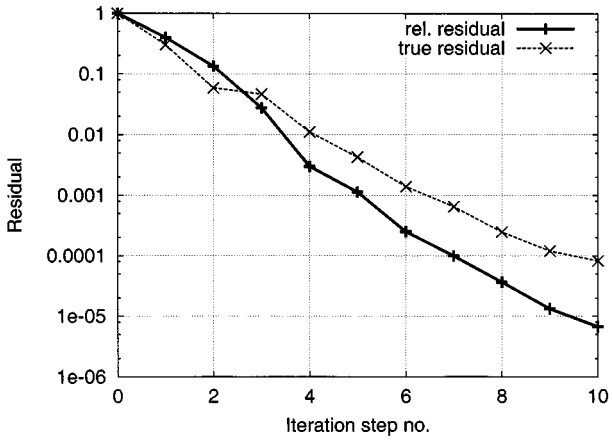

Fig. 6. Comparison of true and relative residual.

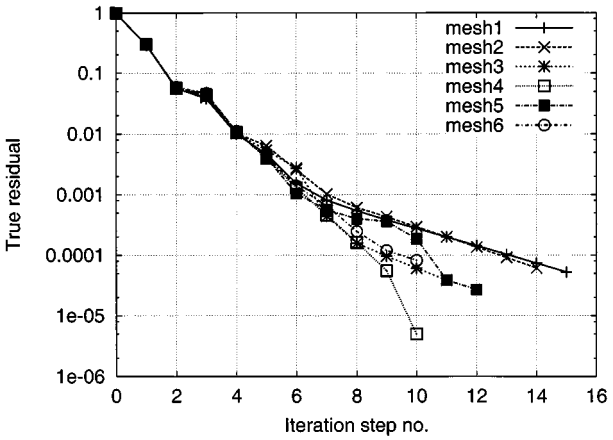

Fig. 7. Convergence rates of different mesh sizes.

rebuild of the system matrix $\mathbf{A}$. But, in this application, the relative residual tends to converge faster, as shown in Fig. 6. Therefore, the termination condition must be one magnitude lower.

B. Convergence Improvement

To improve convergence, an approach with a provided solution is conducted. This initial solution is obtained by solving the problem on meshes with a much lower density. Since the strip is modeled as a simple rectangle 2-D triangular FE mesh with first-order elements, the strip region can be remeshed and the obtained solution transferred to the original denser mesh by interpolation. Fig. 7 shows the convergence rate of the test meshes with different sizes from Table I. It can be seen that the convergence rate of *mesh1* and *mesh2* declines, since the mesh density is not suitable for this problem. The typical mesh size for the calculation of the strip temperature of TFIH device is about 50 000 elements. So the mesh which should provide the initial solution must not be undersized. In Fig. 8, the true residual over the iteration step number is displayed. The curves *mesh4* and *mesh6* represent the convergence rate of the problems with a zero initial solution. If the solution of *mesh4* is provided as the initial solution for *mesh6*, the convergence rate behaves as in curve *mesh4/6*. The size of *mesh4* is four times smaller than the size of *mesh6*. The computation time for *mesh4* is considerably lower, as shown in Table I, since the order of one nonlinear

TABLE I
DIFFERENT TEST MESHES

mesh	no. of elements	time in s	no. of n.l. steps
mesh1	2175	1.4	16
mesh2	4330	3.1	15
mesh3	8725	6.2	12
mesh4	17352	15.5	11
mesh5	34894	48.8	13
mesh6	69346	119.7	11

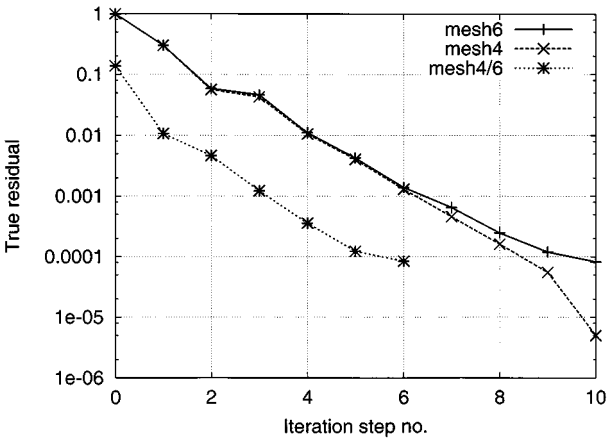

Fig. 8. Convergence rate if a good initial solution is provided.

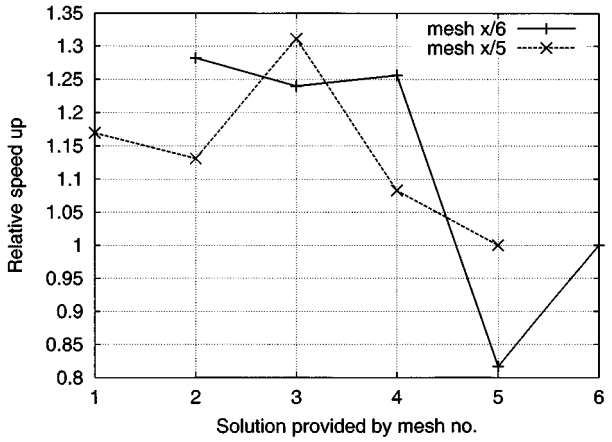

Fig. 9. Relative speedup for different initial solutions.

step is $O(n^{1.59})$, which is near the theoretical order of the BICG algorithm ($O(n^{3/2})$).

An overview of the influence of the initial solution from different sized meshes is presented in Fig. 9. The sum of the computation times for the small and the large mesh are related to the time of the large mesh only. As depicted, the speedup factor is always over one, if the small mesh size is one quarter or less of large mesh. The best speedup factor up to 1.3 is reached by using the eight times smaller mesh as the provider for the initial solution. In general, the speedup factor depends on the problem, caused by the quality of the interpolation of the small mesh solution to the larger mesh. The achievable speedup may increase, if nested meshes or better interpolation algorithms than the applied linear interpolation are used.

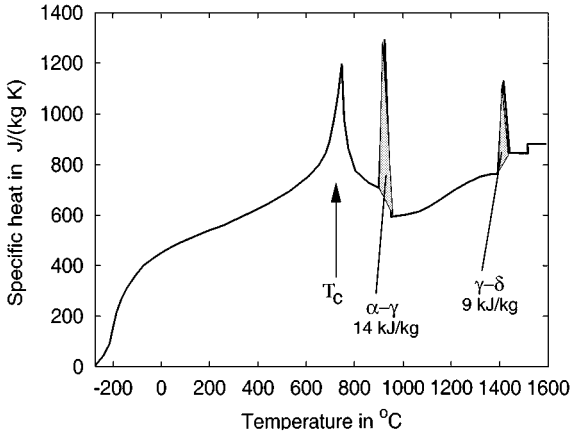

Fig. 10. Specific heat of pure iron modified with phase change energies.

TABLE II
PHASE CHANGE ENERGIES OF PURE IRON

phase change	temperature in °C	energy in $\frac{kJ}{kg}$
$\alpha - \gamma$	905	14.6
$\gamma - \delta$	1391	9.2
solidus/liquidus	1514	276.3

VI. INFLUENCE OF PHASE CHANGE ENERGIES

The influence of latent heat at phase changes is negligible for pure iron: a specific energy of 597 kJ/kg is needed to heat iron from 20 °C to 905 °C. The $\alpha - \gamma$ change requires a latent heat of 14.6 kJ/kg (see Table II, [4]), which is only 2.4%. But this fact may not be true for other steel alloys. Therefore, a more general approach is presented in Fig. 10. Since the area under the specific heat curve is equivalent to the internal energy Q of the material, the latent heat at the phase changes can be taken into account by modifying the curve. The latent heat is converted in an equivalent triangular area, which is added on top of the original curve at the phase change temperatures. As expected, the convergence rate is better if the material does not require this method.

VII. VERIFICATION

An analytical verification has been performed, where a constant heat source density has been applied onto the strip. The influences of heat conduction, convection and radiation have been disabled. Thus, the external applied specific energy can be compared to the integral of the specific heat from strip entry temperature to the exit temperature. The specific energy of the strip differs only by 0.3%, which is negligible.

VIII. CONCLUSION

A method for solving temperature problems with highly nonlinear materials, which are used in a TFIH device, has been presented. The method has been compared to the NR method. Convergence improvements can be reached by providing a good initial solution. This initial solution should be calculated on a four to eight times coarser FE mesh to reduce the overall computation time by 30%. The phase change energies can also be taken into account by modifying the material properties accordingly. Analytical verification of this modification has been performed. The presented method has been found to be a very robust method in this type of application.

REFERENCES

[1] W. Mai and G. Henneberger, "Field and temperature calculations in transverse flux inductive heating device heating nonparamagnetic materials using surface impedance formulations for nonlinear eddy-current problems," *IEEE Trans. Magn.*, vol. 35, no. 3, pp. 1590–1593, May 1999.

[2] W. Bleck and G. Henneberger, *et al.*, "Pilotanlage zum kontinuierlichen Glühen von Stahlband," in *Stahl+Eisen*. Düsseldorf, Germany: Stahleisen, Aug. 2000, pp. 79–85.

[3] G. Payre, *et al.*, "An upwind finite element method via numerical integration," *Int. J. Numerical Methods in Engineering*, vol. 18, pp. 381–396, 1982.

[4] R. Bozorth, *Ferromagnetism*. New York: IEEE Press, 1993, pp. 729–744.